

## Observation of $J/\psi$ Radiative Decay to Pseudoscalar $\omega\omega$

R. M. Baltrusaitis, J. J. Becker, G. T. Blaylock, J. S. Brown, K. O. Bunnell, T. H. Burnett, R. E. Cassell, D. Coffman, V. Cook, D. H. Coward, H. Cui, C. Del Papa, D. E. Dorfan, A. L. Duncan, K. F. Einsweiler, B. I. Eisenstein, R. Fabrizio, G. Gladding, F. Grancagnolo, R. P. Hamilton, J. Hauser, C. A. Heusch, D. G. Hitlin, L. Köpke, P. M. Mockett, L. Moss, R. F. Mozley, A. Nappi, A. Odian, R. Partridge, J. Perrier, S. A. Plaetzer, J. D. Richman, J. R. Roehrig, J. J. Russell, H. F. W. Sadrozinski, M. Scarlatella, T. L. Schalk, R. H. Schindler, A. Seiden, J. C. Sleeman, A. L. Spadafora, J. J. Thaler, W. Toki, Y. Unno, F. Villa, A. Wattenberg, N. Wermes, H. J. Willutzki, D. Wisinski, and W. J. Wisniewski

(Mark III Collaboration)

*California Institute of Technology, Pasadena, California 91125*  
*University of California at Santa Cruz, Santa Cruz, California 95064*  
*University of Illinois at Urbana-Champaign, Urbana, Illinois 61801*  
*Stanford Linear Accelerator Center, Stanford, California 94305*  
*University of Washington, Seattle, Washington 98195*

(Received 15 July 1985)

We present evidence for the radiative decay  $J/\psi \rightarrow \gamma\omega\omega$  with a branching fraction of  $(1.76 \pm 0.09 \pm 0.45) \times 10^{-3}$ . The  $\omega\omega$  invariant-mass distribution peaks at  $1.8 \text{ GeV}/c^2$ , just above threshold. Analysis of angular correlations indicates that the  $\omega\omega$  system below  $2 \text{ GeV}/c^2$  is predominantly pseudoscalar. Upper limits are presented for the branching fractions of  $\omega\omega$  decays of the  $\theta(1690)$ , the  $g_T$  states near  $2.2 \text{ GeV}/c^2$ , and the  $\eta_c$ .

PACS numbers: 13.40.Hq, 13.25.+m, 14.40.Gx

Final states of two vector particles have been intensively studied for signatures of gluonic bound states in the mass region below  $3 \text{ GeV}/c^2$ . Enhancements in  $\rho\rho$  final states have been seen in hadronic interactions,<sup>1</sup> in photon-photon collisions,<sup>2</sup> and in radiative decays of the  $J/\psi$ .<sup>3</sup> In  $\pi^-p$  scattering resonant behavior is observed near threshold in  $\phi\phi$  final states.<sup>4</sup> These structures may be bound states of quarks and gluons, such as  $q\bar{q}$ ,  $qq\bar{q}\bar{q}$ ,  $q\bar{q}g$ , or  $gg$ . Models for some of these hypotheses also predict specific cross sections and rates for decays to  $\omega\omega$ ,<sup>5</sup> although this final state has not previously been observed.

We report a measurement of the branching ratio of the decay  $J/\psi \rightarrow \gamma\omega\omega$ ,  $\omega \rightarrow \pi^+\pi^-\pi^0$ , and a spin and parity analysis of the  $\omega\omega$  system, based on a sample of  $(2.71 \pm 0.16) \times 10^6$  produced  $J/\psi$ 's obtained with the Mark III detector<sup>6</sup> at the SLAC  $e^+e^-$  storage ring SPEAR. For this analysis, the central drift chamber, which measures momenta of charged tracks with a resolution  $\sigma_p/p$  of 2% at  $1 \text{ GeV}/c$  over 84% of the solid angle, and the electromagnetic shower counters are used. The shower counters cover 94% of the solid angle and detect photons with an energy resolution  $\sigma_E/E$  of 17%  $[E (\text{GeV})]^{1/2}$  and with 100% detection efficiency for energies greater than 100 MeV.

Events of the type  $J/\psi \rightarrow \gamma + 2(\pi^+\pi^-\pi^0)$  are selected by the requirement of exactly four charged particles in the drift chamber with zero total charge. Events are also required to have between five and seven detected showers with energies greater than 10 MeV. These showers are required to be outside a cone of half-angle  $18^\circ$  around charged particles, in order to reduce the number of spuri-

ous low-energy photons produced by secondary hadronic interactions. Six-constraint kinematic fits by the hypothesis  $J/\psi \rightarrow \gamma + 2(\pi^+\pi^-\pi^0)$  are then applied, with all possible photon combinations. The combination with the best fit is retained, if the  $\chi^2$  probability is greater than 0.02. Figure 1 shows the distribution of invariant  $\pi^+\pi^-\pi^0$  masses with eight possible combinations per event. The dominant contribution to the  $\omega$  signal comes from  $J/\psi \rightarrow \omega\pi^+\pi^-\pi^0$ .

To reduce further the background, events with spurious photons are rejected if a fit by the background hypothesis  $J/\psi \rightarrow 7\pi$  has a larger  $\chi^2$  probability than the fit by the signal hypothesis, or if the event contains one or more additional photons with detected energies greater than 80 MeV. To remove background events in which a  $\pi^0$  is falsely reconstructed from a high-energy photon and a

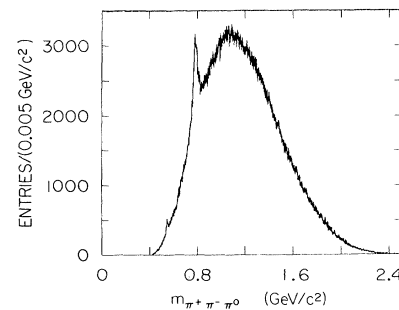


FIG. 1. Three-pion invariant-mass distributions (eight entries per event).

second spurious shower, a cut  $|(E_{\gamma_1} - E_{\gamma_2})/E_{\pi^0}| < 0.9$  is introduced for both  $\pi^0$ 's. Finally, the cut on the  $\chi^2$  probability is increased from 0.02 to 0.15.

The four pairs of  $\pi^+\pi^-\pi^0$  mass combinations per event are plotted in the two-dimensional histogram of Fig. 2. A cluster of events is observed in which both three-pion combinations have an invariant mass equal to  $m_\omega$ . Because the processes  $J/\psi \rightarrow \omega\omega$  and  $J/\psi \rightarrow \pi^0\omega\omega$  are forbidden by  $C$  invariance, the presence of two  $\omega$ 's is direct evidence for the radiative decay  $J/\psi \rightarrow \gamma\omega\omega$ . Figure 3(a) shows the  $6\pi$  invariant-mass distribution for the 412 events in which at least one combination has both  $\pi^+\pi^-\pi^0$  masses within 0.753–0.813  $\text{GeV}/c^2$ . The distribution peaks at 1.8  $\text{GeV}/c^2$  and is approximately 0.250  $\text{GeV}/c^2$  wide.

An estimate of the background in Fig. 3(a) must consider sources from  $J/\psi \rightarrow \gamma 6\pi$ ,  $J/\psi \rightarrow 7\pi$ , and  $J/\psi \rightarrow \omega 4\pi$ . There is also background from the signal process itself when a photon from a  $\pi^0$  decay is undetected, but the event is retained in the sample as a result of spurious showers. To estimate the contributions of these backgrounds to the events in Fig. 3(a), we fit to  $\pi^+\pi^-\pi^0$  distributions of events with one and no  $\omega$  separately and extrapolate the backgrounds into the  $\omega\omega$  signal area. The sum of all backgrounds accounts for  $(35 \pm 7)\%$  of the events below 2  $\text{GeV}/c^2$ . Since the background is largest at low  $\omega\omega$  masses ( $m_{\omega\omega}$ ), alternative methods have been employed to study the contributions of the individual background sources and to verify that the estimation of their magnitude is correct. The dominant contribution,  $(22 \pm 6)\%$ , comes from events which contain one real  $\omega$ . The shaded band in Fig. 3(a) represents all backgrounds; its width reflects both statistical and systematic uncertainties. The purely combinatorial background from events containing more than one combination of pions in the  $\omega\omega$  window,  $(4.9 \pm 1.1)\%$ , does not contribute to Fig. 3(a).

The  $\gamma\omega\omega$  detection efficiency is  $(5.3 \pm 1.1)\%$ , independent of  $m_{\omega\omega}$ . This results in branching fractions of

$$B(J/\psi \rightarrow \gamma\omega\omega) = (1.76 \pm 0.09 \pm 0.45) \times 10^{-3}$$

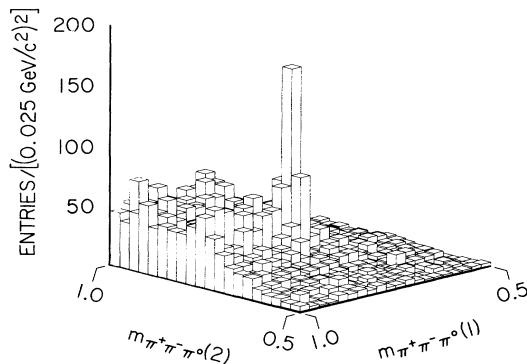


FIG. 2.  $m_{\pi^+\pi^-\pi^0}$  vs  $m_{\pi^+\pi^-\pi^0}$  of the recoiling three-pion system (four entries per event).

for  $m_{\omega\omega} < 3.1 \text{ GeV}/c^2$ , and

$$B(J/\psi \rightarrow \gamma\omega\omega) = (1.22 \pm 0.07 \pm 0.31) \times 10^{-3}$$

for  $m_{\omega\omega} < 2.0 \text{ GeV}/c^2$ . The systematic error includes the uncertainty in the background subtraction. Variation of the photon-acceptance cuts produces no significant change in the branching fractions.  $B(J/\psi \rightarrow \gamma\omega\omega)$  as a function of  $m_{\omega\omega}$  is shown in Fig. 3(b). The three-body phase-space distributions for  $J/\psi \rightarrow \gamma\omega\omega$  for  $S$ -wave and  $P$ -wave  $\omega\omega$  systems are also shown for comparison.

The  $\omega\omega$  invariant-mass distribution in the  $\eta_c$  mass region is shown in the inset of Fig. 3(a). The superimposed curve corresponds to the 90%-confidence-level upper limit of  $B(\eta_c \rightarrow \omega\omega) < 3.1 \times 10^{-3}$  with use of<sup>7</sup>  $B(J/\psi \rightarrow \gamma\eta_c) = (1.27 \pm 0.36) \times 10^{-2}$ .

For the following spin and parity studies, we require that only one of the four  $6\pi$  permutations has both  $\pi^+\pi^-\pi^0$  masses in the  $\omega$  window ( $0.753 < m_{3\pi} < 0.813 \text{ GeV}/c^2$ ). This eliminates 5% of the events. For systems of two vector mesons, the distribution of  $\chi$ , the angle between the meson decay planes, provides a unique signature for spin and parity.<sup>8</sup> This distribution takes the form  $dN/d\chi \propto 1 + \beta \cos(2\chi)$ , where  $\beta$  is a constant which depends only on spin and parity and is independent of the polarization of the  $\omega\omega$  system.  $\beta$  is zero for odd spin and nonzero for even spin. Its sign is the parity of the  $\omega\omega$  system. For  $J^P = 0^-$ , where  $\beta$  is  $-1$ ,  $dN/d\chi \propto \sin^2\chi$ , and the effect is maximal.

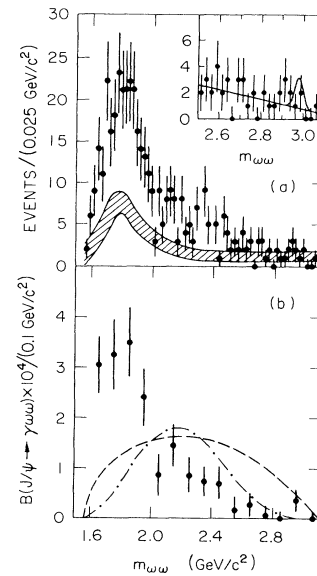


FIG. 3. (a)  $\omega\omega$  invariant-mass distribution (one entry per event). The shaded band displays the background contribution. The inset shows the  $\eta_c$  mass region. (b)  $B(J/\psi \rightarrow \gamma\omega\omega)$  as a function of  $m_{\omega\omega}$ . The errors include the uncertainty of the background subtraction, but not an overall systematic error of 16%.  $S$ -wave (dashed) and  $P$ -wave (dot-dashed) phase-space distributions are indicated.

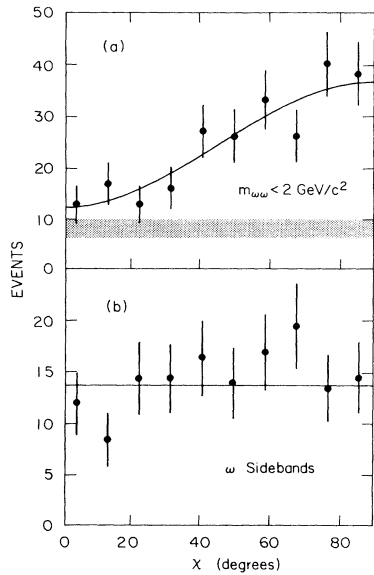


FIG. 4. Distribution of  $\chi$ , the angle between the  $\omega$  decay planes (a) for  $m_{\omega\omega} < 2 \text{ GeV}/c^2$  and (b) for  $\omega$  sideband events. The curves are fits with (a)  $a + b \sin^2\chi$ , and (b) a constant. The magnitude of a flat background is indicated by the band in (a).

Figure 4 shows the  $\chi$  distribution for (a)  $J/\psi \rightarrow \gamma\omega\omega$  with  $m_{\omega\omega}$  less than  $2 \text{ GeV}/c^2$ , and (b) events from the  $\omega$  sidebands ( $0.723 < m_{\omega} < 0.753 \text{ GeV}/c^2$  and  $0.813 < m_{\omega} < 0.843 \text{ GeV}/c^2$ ). The distributions for signal and background events are strikingly different, the signal indicating a large component with even spin and odd parity. The solid line in Fig. 4(a) is the result of a fit with  $a + b \sin^2\chi$ , which yields a  $\sin^2\chi$  contribution for the  $\gamma\omega\omega$  event candidates below  $2 \text{ GeV}/c^2$  of  $(75 \pm 16)\%$ , when we correct for the presence of a flat background, as indicated in the figure.

A multichannel analysis of the  $\omega\omega$  final state is performed which allows for six possible spin and parity contributions to the  $\omega\omega$  system,  $0^\pm$ ,  $1^\pm$ , and  $2^\pm$ , plus an isotropic contribution.<sup>9</sup> The following assumptions are made to restrict the number of parameters: (a) Only the lowest orbital angular momentum is considered for a given spin and parity, (b) the ratios of helicity amplitudes  $x = A_1/A_0$  and  $y = A_2/A_0$ , although free parameters in the fit, are assumed to be real,<sup>10</sup> and (c) interference between amplitudes of different spin and parity channels is not considered.

The number of events contributing to each of the seven channels as determined by the fit is displayed in Figs. 5(a)–5(g) as a function of  $m_{\omega\omega}$ . The distribution of background events, obtained by application of the same method to  $\omega$  sideband events, is indicated by the dashed histogram lines. The dominant feature at masses below  $2 \text{ GeV}/c^2$  appears in the  $0^-$  channel, amounting to  $(55 \pm 11)\%$  of the events,  $\gamma\omega\omega$  plus background. This corresponds to  $(85 \pm 19)\%$  of the  $\gamma\omega\omega$  signal, since the

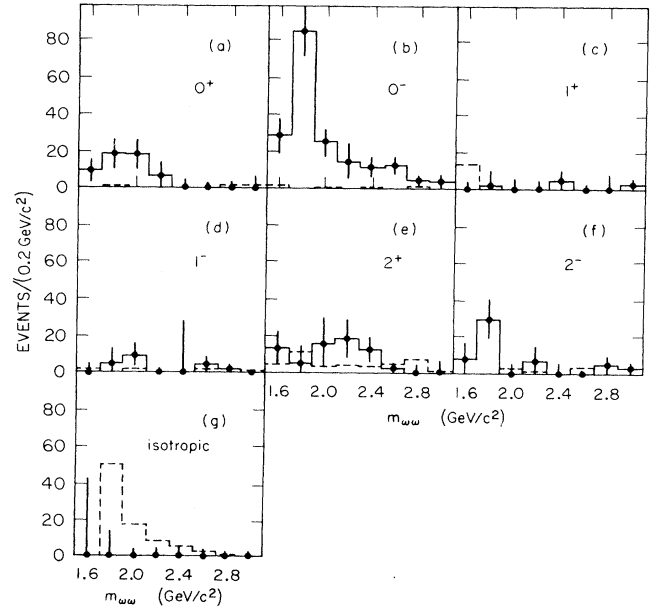


FIG. 5. Results of the seven-channel spin and parity analysis. The background contributions are indicated by the dashed histogram lines.

background (35%) is found not to contribute to this channel. This is consistent with the result obtained by the  $\chi$ -angle analysis. Events from the sidebands largely populate the isotropic channel. We conclude that the  $\omega\omega$  signal below  $2 \text{ GeV}/c^2$  is predominantly  $0^-$  spin and parity.

From the contributions to the  $2^+$  channel [Fig. 5(e)] we estimate the 90%-confidence-level upper limits for the  $2^{++}$  meson  $\theta(1690)$ <sup>11</sup> and the tensor states observed in  $\pi^-p \rightarrow \phi\phi n$  reactions<sup>4</sup>:

$$B(J/\psi \rightarrow \gamma\theta)B(\theta \rightarrow \omega\omega) < 2.4 \times 10^{-4},$$

$$B(J/\psi \rightarrow \gamma g_T)B(g_T \rightarrow \omega\omega) < 2.6 \times 10^{-4}.$$

Here  $g_T$  stands for the mass range  $2.1 \leq m_{\omega\omega} \leq 2.4 \text{ GeV}/c^2$ .

In summary, we have observed the decay  $J/\psi \rightarrow \gamma\omega\omega$ ,  $\omega \rightarrow \pi^+\pi^-\pi^0$ , in which the  $\omega\omega$  system below  $2 \text{ GeV}/c^2$  is found to be predominantly  $0^-$  spin and parity. The  $\omega\omega$  mass distribution peaks at  $1.8 \text{ GeV}/c^2$ , which may be the result of a combination of rising phase space and falling amplitude due to resonances below threshold, specifically the  $\iota(1440)$ .<sup>12</sup> An analysis to correlate this with similar behavior found<sup>9</sup> in  $J/\psi \rightarrow \gamma\rho\rho$  is in progress.

We wish to acknowledge the efforts of the SPEAR staff. One of us (N.W.) wishes to thank the Alexander von Humboldt Foundation for support. This work was supported in part by the U.S. Department of Energy, Contracts No. DE-AC03-76SF00515, No. DE-AC02-76ER01195, No. DE-AC03-81ER40050, and No. DE-AM03-76SF00034, and by the National Science Foundation.

- <sup>1</sup>A. Bettini *et al.*, *Nuovo Cimento* **42**, 695 (1966); H. Braun *et al.*, *Nucl. Phys.* **B30**, 213 (1971).
- <sup>2</sup>R. Brandelik *et al.*, *Phys. Lett.* **97B**, 448 (1980); M. Althoff *et al.*, *Z. Phys. C* **16**, 13 (1982); D. L. Burke *et al.*, *Phys. Lett.* **103B**, 153 (1981); H. J. Behrend *et al.*, *Z. Phys. C* **21**, 205 (1984).
- <sup>3</sup>D. L. Burke *et al.*, *Phys. Rev. Lett.* **49**, 632 (1982).
- <sup>4</sup>A. Etkin *et al.*, *Phys. Rev. Lett.* **49**, 1620 (1982).
- <sup>5</sup>B. A. Li and K. F. Liu, *Phys. Rev. D* **30**, 613 (1984).
- <sup>6</sup>D. Bernstein *et al.*, *Nucl. Instrum. Methods* **226**, 301 (1984).
- <sup>7</sup>R. Partridge *et al.*, *Phys. Rev. Lett.* **45**, 1150 (1980).
- <sup>8</sup>N. P. Chang and C. T. Nelson, *Phys. Rev. Lett.* **40**, 1617 (1978); T. L. Trueman *et al.*, *Phys. Rev. D* **18**, 3423 (1978); R. M. Baltrusaitis *et al.*, *Phys. Rev. Lett.* **52**, 2126 (1984).
- <sup>9</sup>R. M. Baltrusaitis *et al.*, SLAC Report No. SLAC-PUB-3682, 1985 (to be published).
- <sup>10</sup>This assumption is found to be well fulfilled for the decays  $J/\psi \rightarrow \gamma f(1270)$ ,  $f \rightarrow \pi^+ \pi^-$ , and  $J/\psi \rightarrow \gamma f'(1515)$ ,  $f' \rightarrow K^+ K^-$ ; R. M. Baltrusaitis *et al.*, SLAC Report No. SLAC-PUB-3720, 1985 (to be published).
- <sup>11</sup>C. Edwards *et al.*, *Phys. Rev. Lett.* **48**, 458 (1982).
- <sup>12</sup>N. N. Achasov and G. N. Shestakov, Institute of Theoretical Physics, Siberian Division of the Institute of Mathematics, Academy of Sciences, U.S.S.R. Report No. TF-83-142, 1985 (to be published).